**Author(s):** Hossain, Md Kamal; Köhntopp, Anja; Haukka, Matti; Richmond, Michael G.; Lehtonen, Ari; Nordlander, Ebbe

**Title:** Cis- and trans molybdenum oxo complexes of a prochiral tetradentate aminophenolate ligand : Synthesis, characterization and oxotransfer activity

**Year:** 2020

**Version:** Accepted version (Final draft)



**Please cite the original version:**

Hossain, M. K., Köhntopp, A., Haukka, M., Richmond, M. G., Lehtonen, A., & Nordlander, E. (2020). Cis- and trans molybdenum oxo complexes of a prochiral tetradentate aminophenolate ligand : Synthesis, characterization and oxotransfer activity. Polyhedron, 178, Article 114312. https://doi.org/10.1016/j.poly.2019.114312

Journal Pre-proofs

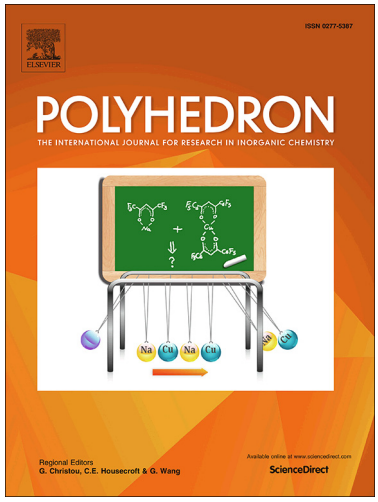


*Cis*- and *trans* molybdenum oxo complexes of a prochiral tetradentate aminophenolate ligand: Synthesis, characterization and oxotransfer activity

Md. Kamal Hossain, Anja Köhntopp, Matti Haukka, Michael G. Richmond, Ari Lehtonen, Ebbe Nordlander

PII: S0277-5387(19)30757-0
DOI: https://doi.org/10.1016/j.poly.2019.114312
Reference: POLY 114312

To appear in: *Polyhedron*

Received Date: 19 September 2019
Revised Date: 12 December 2019
Accepted Date: 15 December 2019

Please cite this article as: Md. Kamal Hossain, A. Köhntopp, M. Haukka, M.G. Richmond, A. Lehtonen, E. Nordlander, *Cis*- and *trans* molybdenum oxo complexes of a prochiral tetradentate aminophenolate ligand: Synthesis, characterization and oxotransfer activity, *Polyhedron* (2019), doi: https://doi.org/10.1016/j.poly.2019.114312

# *Cis*- and *trans* molybdenum oxo complexes of a prochiral tetradentate aminophenolate ligand: Synthesis, characterization and oxotransfer activity

**Md. Kamal Hossain,[a,b] Anja Köhntopp,[a] Matti Haukka,[c] Michael G. Richmond,[d] Ari Lehtonen[e,*], Ebbe Nordlander [a,*]**

a. Chemical Physics, Department of Chemistry, Lund University, P.O. Box 124, SE-22100 Lund, Sweden
b. Department of Chemistry, Jahangirnagar University, Savar, Dhaka-1342, Bangladesh
c. Department of Chemistry, P.O. Box 35, University of Jyväskylä, FI-40014 Jyväskylä, Finland
d. Department of Chemistry, University of North Texas, 1155 Union, Circle#305070, Denton, TX 76203, USA
e. Laboratory of Materials Chemistry and Chemical Analysis, Department of Chemistry, University of Turku, FI-20014 Turku, Finland

* Corresponding authors
E-mail: ari.lehtonen@utu.fi (A. Lehtonen), ebbe.nordlander@chemphys.lu.se (E. Nordlander).

## REVISED MANUSCRIPT

ABSTRACT

Reaction of $[MoO_2Cl_2(dmso)_2]$ with the tetradentate $O_2N_2$ donor ligand papy [$H_2$papy = *N*-(2-hydroxybenzyl)-*N*-(2-picolyl)glycine] leads to formation of the dioxomolybdenum(VI) complex $[MoO_2(papy)]$ (**1**) as a mixture of *cis* and *trans* isomers. Recrystallization from methanol furnishes solid *cis*-**1**, whereas the use of a dichloromethane-hexane mixture allows for the isolation of the *trans*-**1** isomer. Both isomers have been structurally characterized by X-ray crystallography and the energy difference between the isomeric pair has been investigated by electronic structure calculations. Optimization of two configurational isomers in the gas phase predicts the *trans* isomer to lie 2.5 kcal/mol lower in energy (ΔG) than the *cis* isomer, which is inconsistent with the solution NMR data in $d_3$-MeCN that exhibit a $K_{eq}$ of *ca*. 3 at 298 K for the *trans*⇌*cis* equilibrium. The DFT-computed energy difference is significantly improved ($K_{eq}$ = 5.4) by the inclusion of the MeCN solvent using the polarization continuum model (PCM). Density functional calculations reveal that the isomerization proceeds via a Ray-Dutt twist mechanism with a barrier of 14.5 kcal/mol, which is in accordance with the $^1$H NMR spectral data and the rapid equilibration of these isomers in solution. The catalytic reactivity of $[MoO_2(papy)]$ in the epoxidation of *cis*-cyclooctene is described, as well as its ability to effect oxo transfer from DMSO to $PPh_3$.

**Keywords:** Oxo Atom Transfer • Epoxidation • Tripodal Ligand • Variable Temperature NMR • Computational Modelling

## 1. Introduction

High-valent molybdenum complexes containing a *cis*-$MoO_2$ unit have attracted considerable interest due to their applications in a variety of catalytic oxotransfer reactions [1-5]. In particular, these complexes are known to catalyse various industrially valuable processes, *e.g*. (asymmetric) alkene epoxidation and alcohol oxidation. In the catalytic epoxidation of alkenes effected by molybdenum complexes, $O_2$, $H_2O_2$ or *tert*-butylhydroperoxide (TBHP), are typically used as oxidants [6-8]. An example of an industrial process employing a molecular Mo(VI) oxo catalyst is the Halcon process for oxidation of propylene to propylene oxide by TBHP [9]. Propylene oxide is an important building block in the synthesis of polyurethane, and other relatively simple epoxides are used in the synthesis of polyglycols, fine chemicals and food additives [10]; it is a chiral molecule that is usually used as a racemate, and asymmetric epoxidation catalysis effected by molybdenum catalysts remains a significant challenge [11,12]. *Cis*-$MoO_2$ complexes with different ligands have also been studied as soluble molecular models for metal oxide catalysts [13,14].

Molybdenum is also a necessary element in diverse biological systems, where molybdenum-containing active sites are found in numerous redox enzymes [15]. Such molybdopterin-dependent enzymes play key roles in living organisms and are involved in essential steps in the biological sulfur- and nitrogen cycles, where they catalyse oxygen atom transfer (OAT) reactions consisting of the transfer of an oxygen atom to or from a biologically relevant acceptor/donor molecule [16,17]. Thus, a number of dioxomolybdenum(VI) complexes have been studied as models for oxidized forms of molybdenum-containing oxidoreductases that contain Mo(VI)X units (X=O, S) coordinated by at least one dithiolene unit of a molybdopterin [18-25].

High oxidation state complexes of molybdenum are dominated by species that contain a *cis*-$MoO_2^{2+}$ moiety with a distorted octahedral coordination sphere that is typically completed by two anionic (X) ligands in *trans* positions and two neutral ligands (L) *trans* to the oxo ligands and thus *cis* to each other (Fig. 1a). However, sometimes steric factors and/or the rigidity of the ligand backbone leads to coordination of the ligands in an all-*cis* mode (Fig. 1b) [1,26].

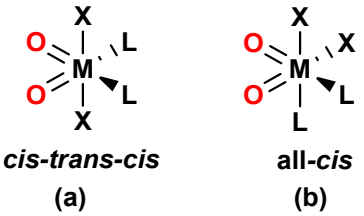


**Fig. 1.** (a) *cis-trans-cis* and (b) all-*cis* coordination modes.

We have studied a number of dioxomolybdenum(VI) and –tungsten(VI) complexes based on multidentate aminophenolate ligands, including their applications as catalysts for oxygen atom transfer/oxidation reactions [27]. Here, we describe the synthesis and characterization of a new *cis*-$MoO_2^{2+}$ complex based on the tripodal ligand *N*-(2-hydroxybenzyl)-*N*-(2-picolyl)glycine ($H_2$papy), a chiral molecule in which the central amine nitrogen becomes a stereogenic center upon coordination. In the solid state, the complex [$MoO_2$(papy)] (**1**) can be isolated as two different configurational isomers, *viz*. *cis-trans-cis* and all-*cis*, depending on the crystallization solvent. The two configurational isomers were fully characterized including single-crystal X-ray diffraction analysis. The ability of **1** to catalyse phosphine oxidation and alkene epoxidation is also described.

## 2. Results and discussion

### *2.1. Syntheses and spectral characterization*

The starting material [$MoO_2Cl_2$(dmso)$_2$] was allowed to react with $H_2$papy in the presence of two equivalents of triethylamine in methanol to obtain a yellow solution from which yellow crystals of [$MoO_2$(papy)] (**1**) were grown upon slow evaporation of the solvent. Solid **1** is moderately soluble in polar solvents, *e.g*. DMSO, $CH_2Cl_2$ and MeOH, to give a clear yellow solution but it is poorly soluble in non-polar solvents. The use of other dioxomolybdenum(VI) precursors, *i.e*. [$MoO_2$(acac)$_2$], [$MoO_2Cl_2$(dmf)$_2$] and [$MoO_2$($S_2NEt_2$)$_2$], led to the formation of an identical product. The $^1$H NMR spectra of the isolated products indicate that in all reactions the product is a mixture of two isomers. In principle, tripodal papy$^{2-}$ may coordinate to the *cis*-$MoO_2^{2+}$ moiety to form three different coordination isomers. One isomer (*trans*-**1** in Fig. 2)* has a *cis-trans-cis* configuration of oxo groups, anionic donors and neutral donors, respectively. For an all-*cis* configuration there are

* Throughout this paper, **1** will refer to the compound mixture of the two configurational isomers *cis*-**1** and *trans*-**1**.

two possible isomers as the pyridyl side-arm donor can be located either *trans* to the phenolate (*cis*-**1** in Fig. 2) or *trans* to the carboxylate group. However, the latter third isomer was not observed. It should be noted that the tertiary amine of the $H_2$papy (papy$^{2-}$) ligand has a stereogenic center, and that racemic mixtures of the configurational isomers are thus expected in all cases.

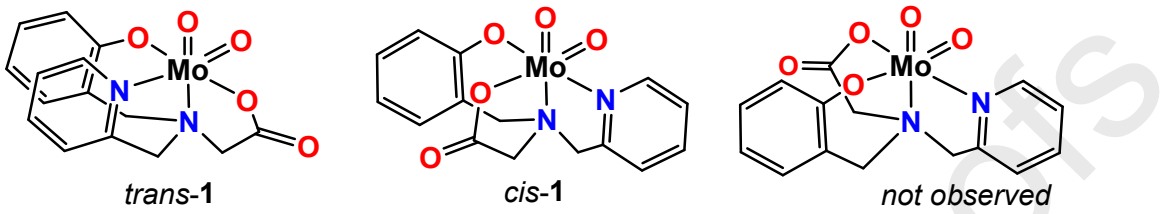


**Fig. 2.** Possible configurational isomers of [$MoO_2$(papy)].

Several attempts were made to isolate different isomers by recrystallization, and the products were analyzed by single-crystal X-ray crystallography. The crystallization of **1** from a methanol solution yielded *cis*-**1** as yellow blocks whereas the use of a dichloromethane-hexane mixture yielded *trans*-**1** as needles. Unexpectedly, the recrystallization from a chloroform-diethyl ether mixture gave needle-shape crystals that were found to contain both *cis* and *trans* isomers in the same asymmetric unit. However, the crystallized, isolated isomers give similar $^1$H NMR spectra with signals attributable to both the *cis*- and *trans*-isomers in approximate 3:1 ratio at room temperature. The use of several deuterated NMR solvents (chloroform, methanol, dimethyl sulfoxide, and acetonitrile) has no visible effect on the *cis*/*trans* ratio. In *cis*-**1**, the pyridyl ring is deshielded due to the phenolate group that is positioned *trans* to the pyridyl ring, while in *trans*-**1**, the pyridyl ring is shielded due to the π-donation from the *trans* oxo ligands. Therefore, the isomer whose pyridyl α-hydrogen appears at lower field in the $^1$H NMR spectrum is assigned to the *cis*-**1** isomer, and the chemical shift assignments of the pyridyl α-hydrogen for both isomers were corroborated by DFT-GIAO NMR calculations. The $^1$H NMR spectra (Fig. 3) reveal that *cis*-**1** is favoured in solution at room temperature. The relative stabilities of the two isomers were probed by variable-temperature $^1$H NMR spectroscopy. At 343K, the *cis*-**1** isomer is the predominant species with a *ca*. 80% population and the equilibrium constants depends on the temperature whereas at low temperatures the percentage decreases very slightly. At 233K, the population of *cis*-**1** is *ca.* 75 %. The relative ratios of integral values for the pyridyl α-hydrogens of the two isomers are shown in Fig. 4.

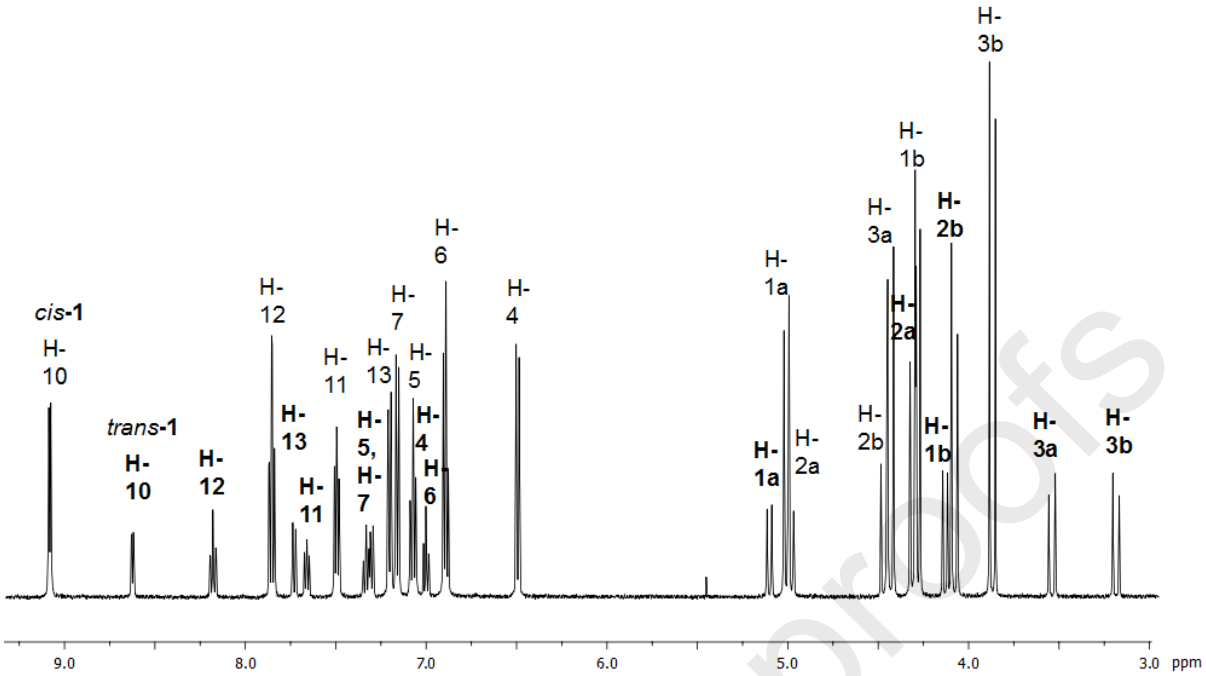


**Fig. 3.** The $^{1}$H NMR spectrum of **1** at room temperature. Bold letters denote resonances assigned to *trans*-**1**.

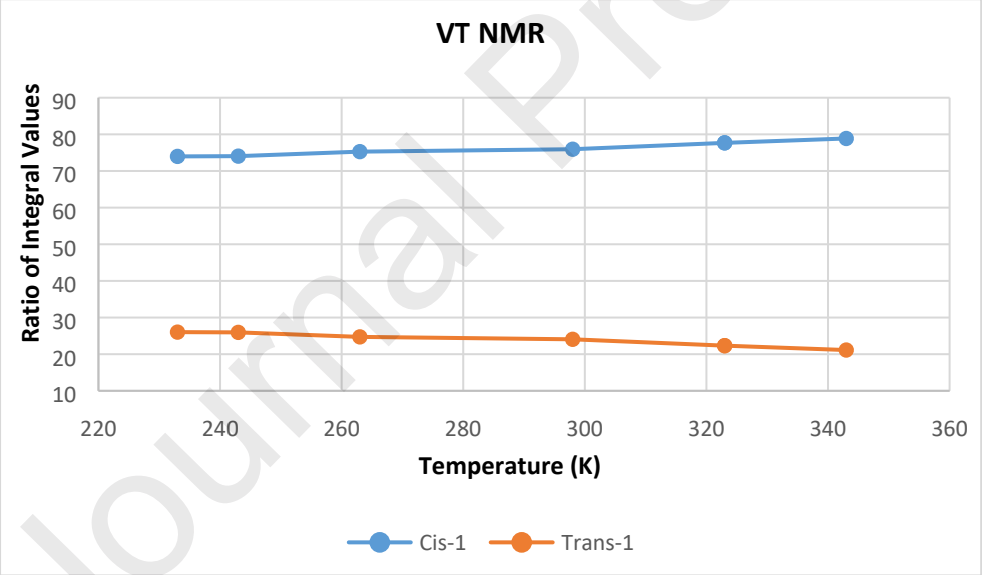


**Fig. 4a.** Ratio of integral values of variable temperature (VT) NMR of **1**.

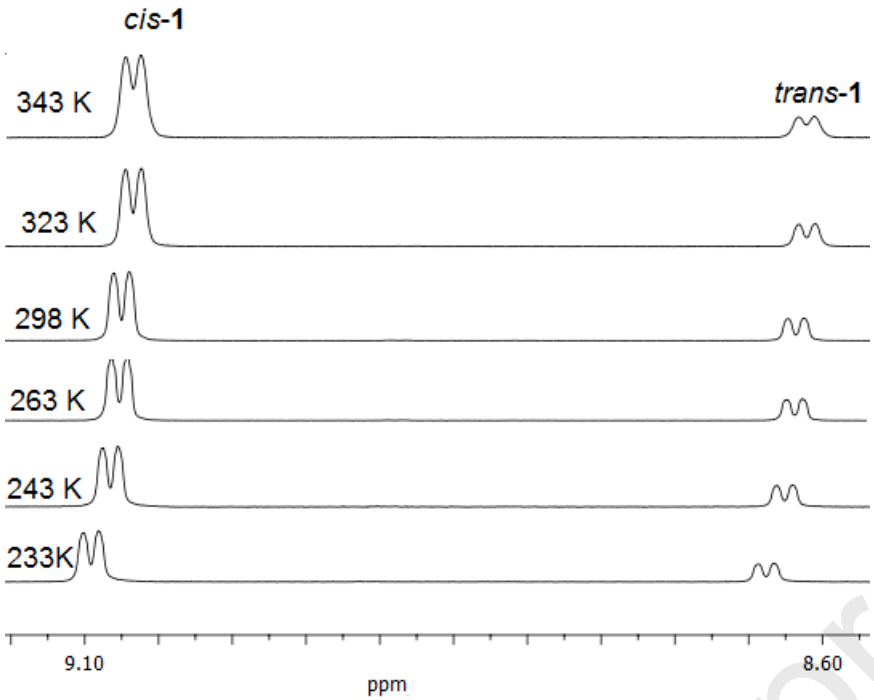


**Fig. 4b.** Variable temperature (VT) NMR of **1** showing the pyridyl α-hydrogen resonances for the two configurational isomers.

The IR spectra of isolated solids show two strong absorptions attributed to the symmetric and asymmetric O=M=O stretches, which are observed around 929 and 916 $cm^{-1}$ but no clear differences between the *cis* and *trans* isomers were seen. The ESI-MS spectrum of either isomer shows three distinct patterns at *m/z* = 823 $[2x\mathbf{1}+Na]^+$, 423 $[\mathbf{1}+Na]^+$ and 401 $[\mathbf{1}+H]^+$ with the expected isotopic distribution.

*2.2. Electronic structure calculations*

The two isomers of **1** were examined by Density Functional Theory (DFT) in order to evaluate the free energy difference between the two configurational isomers of the complex. Gas-phase optimization of the isomeric pair using a range of functionals (**B3LYP**, M06, M062X, ωB97XD, TPSS, and PBE) consistently furnished *trans*-**1** as the thermodynamically favoured species. Use of the correlated *ab initio* Møller-Plesset (MP2) method also confirmed *trans*-**1** as the favoured species in the gas phase. Given the failure of these computations to predict the experimentally observed isomer ratio correctly, we next repeated the calculations in the presence of MeCN solvent using the available polarizable continuum model (PCM) to approximate better the actual environment experienced by each isomer. The use of the M06 as the functional afforded an isomer ratio in best agreement with the NMR data. Here the

optimized structure for *cis*-**1** (**A**) was found to be 1.0 kcal/mol more stable than that of *trans*-**1** (**B**), leading to a $K_{eq}$ of 5.4 for the *trans* ⇌ *cis* equilibrium in close agreement with the $^{1}H$ NMR spectroscopy at room temperature. Fig. 5 shows the optimized structures for **A** and **B**, whose computed bond distances and angles are in keeping with the X-ray diffraction data for each compound.

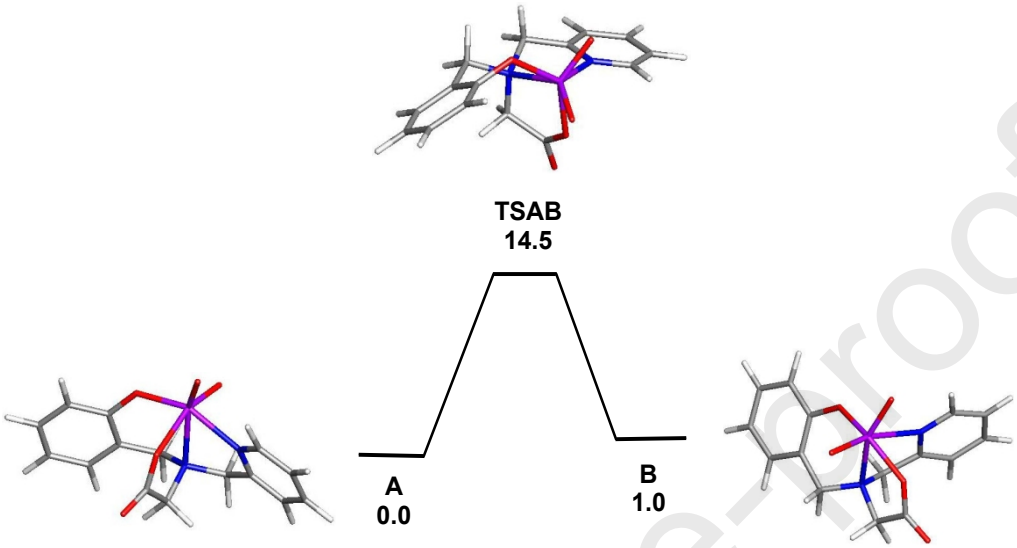


**Fig. 5.** M06-optimized structures and potential energy surface for the isomerization of **A** to **B** via the transition structure **TSAB**. Energy values are ΔG in kcal/mol relative to **A**.

Given the facile equilibration that recrystallized samples of pure *cis*-**1** and *trans*-**1** exhibit when dissolved in solution, we next computationally explored the mechanism for this process. A low-energy process involving transition structure **TSAB** was found, and the computed barrier of 14.5 kcal/mol is consistent with the rapid formation of the two dioxo diastereomers upon dissolution. The equilibration occurs through a Ray-Dutt twist mechanism where the polyhedral face defined by the two oxo ligands and the phenolic oxygen atom twist relative the remaining three atoms ($N_{amine}$, $N_{pyridyl}$, $O_{acetate}$). The optimized structure computed for **TSAB** displays an idealized trigonal prismatic array of the ancillary ligands about the molybdenum center, allowing for the effective oxo exchange about the different sites in the octahedral ground-state structures of **A** and **B**. Fig. 6 illustrates this isomerization reaction.

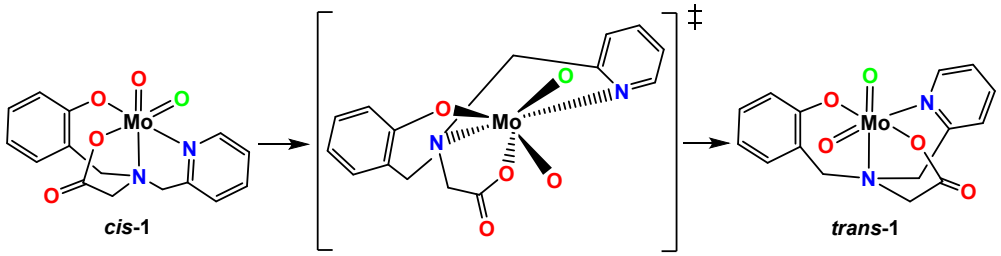


**Fig. 6.** Ray-Dutt twist mechanism involving the isomerization of compound **1**.

*2.3. Solid-state structures of the complexes*

The X-ray quality crystals of *cis*-**1** were obtained from methanol whereas the crystals of *trans*-**1** were grown from a dichloromethane-hexane mixture. Crystals of *cis*/*trans*-**1** (both *cis* and *trans* isomers in the same asymmetric unit) were formed in a chloroform-diethyl ether mixture. The molecular structures for *cis*-**1** and *trans*-**1** are shown in Fig. 7. Relevant crystallographic data are summarized in Table 1 and selected bond lengths and angles for *cis*-**1** and *trans*-**1** are listed in Table 2. As the complex units in the mixed *cis*/*trans*-**1** crystal structure carry the features of both separated isomers, only the solid-state structures of *cis*-**1** and *trans*-**1** are discussed here. The molecular structures of both isomers of **1** reveal a distorted octahedral coordination geometry around the metal centre with two *cis*-positioned oxo ligands bound strongly to the Mo(VI) ion. In *cis*-**1**, the phenoxide and carboxylate oxygen atoms are located in *cis* positions with the O3-Mo1-O4 bond angle being 86.62(10)°, and the pyridyl ring is situated in *trans* position to the phenoxide ring. In *trans*-**1**, the phenoxide and carboxylate oxygen atoms are placed in *trans* positions with the O3-Mo1-O4 angle of 152.80(8)°, with the pyridyl ring in *cis* position relative to the phenoxide ring. In both isomers, the central amine nitrogen of the ligand backbone is coordinated *trans* to the terminal oxo ligand O1. The O1-Mo1-O2 angles are 105.40(12)° and 108.26(10)° for *cis*-**1** and *trans*-**1**, respectively, which are similar to those reported earlier for octahedral molybdenum dioxo complexes [28-31]. The short Mo1-O1 and Mo1-O2 distances (1.701(2) Å - 1.711(2) Å) indicate typical Mo=O bonds. The strong structural *trans* effect of the terminal ligand O2 is seen in both complexes, *i.e.* the carboxylate Mo1-O4 bond length is slightly (0.09 Å) longer for *cis*-**1** than for the *trans*-**1** isomer. Similarly, the pyridyl Mo1-N1 bond length is clearly longer (by 0.17 Å) in *trans*-**1** compared to *cis*-**1**. In general, the bond angles and distances are comparable to those reported earlier for related complexes, *e.g.* the cationic molybdenum dioxo complex of the ligand *N*-(2 hydroxybenzyl)-*N*,*N*-bis(2-pyridylmethyl)amine [32].

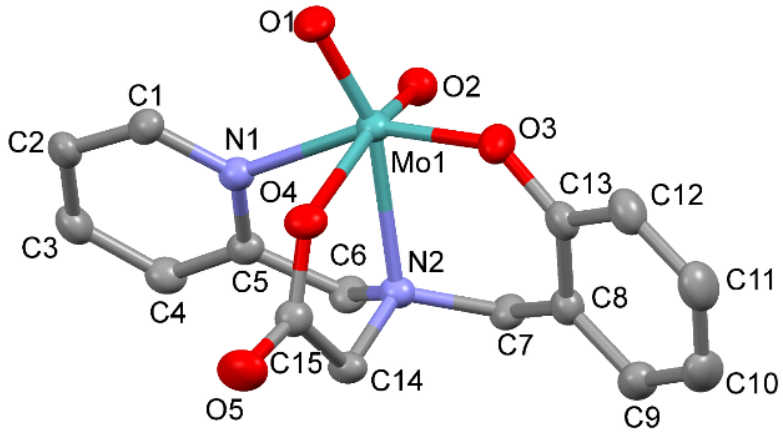


**Fig. 7a.** The solid-state structure of *cis*-**1**. Thermal ellipsoids are drawn at 50% probability level. Hydrogen atoms and solvent molecules are omitted for clarity.

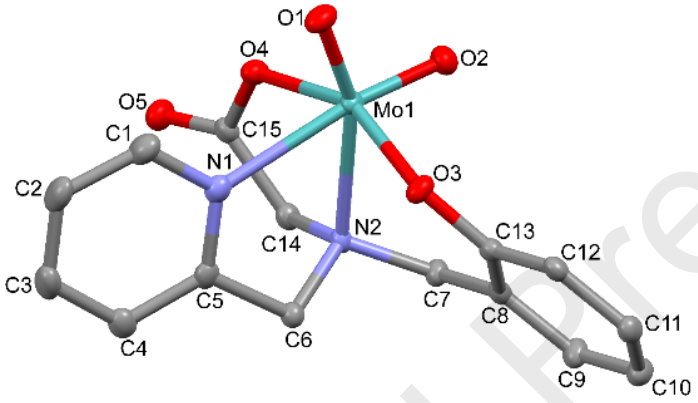


**Fig. 7b.** The solid-state structure of *trans*-**1**. Thermal ellipsoids are drawn at 50% probability level. Hydrogen atoms are omitted for clarity.

**Table 1.** Summary of crystallographic data for complexes *cis*-**1**, *trans*-**1**, and *cis*-*trans*-**1**

| | *cis*-**1** | *trans*-**1** | *cis*-*trans*-**1** |
|---|---|---|---|
| Empirical formula | $C_{15}H_{14}MoN_2O_5 \cdot CH_3OH$ | $C_{30}H_{28}Mo_2N_4O_{10}$ | $C_{30}H_{28}Mo_2N_4O_{10}$ |
| Formula weight | 430.26 | 796.44 | 796.44 |
| Temperature (K) | 170(2) K | 170(2) | 100(2) K |
| Wavelength (Å) | 0.71073 Å | 0.71073 | 0.71073 Å |
| Crystal system | Triclinic | Monoclinic | Triclinic |
| Space group | *P* -1 | $P2_1/n$ | *P* -1 |
| *a* (Å) | 6.9252(5) | 12.2535(4) | 10.5783(2) |
| *b* (Å) | 9.4641(6) | 16.4162(5) | 12.5193(3) |
| *c* (Å) | 13.7217(9) | 15.0553(5) | 12.5227(3) |
| *α* (°) | 106.314(6) | 90 | 100.4077(12) |
| *β* (°) | 103.006(6) | 98.450(3) | 100.8009(14) |
| *γ* (°) | 94.480(5) | 90 | 110.3751(13) |
| Volume (Å$^3$) | 831.32(10) | 2995.57(16) | 1471.66(6) |
| Z | 2 | 4 | 2 |
| Density (calculated) (Mg m$^{-3}$) | 1.719 | 1.766 | 1.797 |
| *μ* (Mo K*α*) (mm$^{-1}$) | 0.825 | 0.903 | 0.919 |
| *F*(000) | 436 | 1600 | 800 |
| Crystal size (mm) | 0.241 x 0.204 x 0.101 | 0.268 x 0.096 x0.037 | 0.203 x 0.134 x 0.129 |
| *θ* range (°) | 2.268 to 30.502 | 2.004 to 30.464 | 1.801 to 30.032 |
| Limiting indices | $-9 \le h \ge 9$<br>$-11 \le k \ge 13$<br>$-19 \le l \ge 12$ | $-16 \le h \ge 14$<br>$-23 \le k \ge 18$<br>$-14 \le l \ge 21$ | $-14 \le h \ge 14$<br>$-17 \le k \ge 17$<br>$-17 \le l \ge 17$ |
| Reflections collected | 7334 | 15998 | 33129 |
| Independent reflections ($R_{int}$) | 4421(0.0430) | 8049 (0.0331) | 8595 (0.0597) |
| Completeness to theta = 25.242° | 100.0 % | 100.0 % | 99.8 % |
| Absorption correction | Semi-empirical from equivalents | Semi-empirical from equivalents | Semi-empirical from equivalents |
| Max. and min. transmission | 1.00000 and 0.78654 | 1.00000 and 0.53884 | 0.8906 and 0.8353 |
| Refinement method | Full-matrix least squares on F2 | Full-matrix least-squares on F2 | Full-matrix least-squares on F2 |
| Data/restraints/parameters | 4421 / 0 / 228 | 8049 / 0 / 415 | 8595 / 0 / 415 |
| Goodness of fit on $F^2$ | 1.078 | 1.024 | 1.037 |
| Final *R* indices [$I > 2\sigma(I)$] | $R_1 = 0.0449$, $wR_2 = 0.0964$ | $R_1 = 0.0394$, $wR_2 = 0.0845$ | $R_1 = 0.0349$, $wR_2 = 0.0746$ |
| R indices (all data) | $R_1 = 0.0563$, $wR_2 = 0.1057$ | $R_1 = 0.0552$, $wR_2 = 0.0927$ | $R_1 = 0.0546$, $wR_2 = 0.0822$ |
| Largest difference in peak and hole (e Å$^{-3}$) | 0.753 and -0.934 | 0.477 and -0.820 | 1.161 and -1.233 |

**Table 2.** Selected bond distances (Å) and angles (°) of *cis*-**1** and *trans*-**1**.

| Bond distances (Å) and angles (°) | *cis*-**1** | *trans*-**1** |
|---|---|---|
| Mo1-O1 | 1.705(2) | 1.7075(19) |
| Mo1-O2 | 1.711(2) | 1.701(2) |
| Mo1-O3 | 1.908(2) | 1.914(2) |
| Mo1-O4 | 2.128(2) | 2.034(2) |
| Mo1-N1 | 2.205(3) | 2.355(2) |
| Mo1-N2 | 2.348(3) | 2.345(2) |
| O1-Mo1-O2 | 105.40(12) | 108.26(10) |
| O1-Mo1-O3 | 107.12(12) | 101.21(9) |
| O1-Mo1-O4 | 90.40(10) | 96.68(9) |
| O2-Mo1-O4 | 159.03(11) | 94.08(10) |
| O3-Mo1-O4 | 86.62(10) | 152.80(8) |
| O1-Mo1-N1 | 92.21(11) | 87.06(9) |
| O1-Mo1-N2 | 158.80(10) | 157.77(10) |
| O2-Mo1-N1 | 86.34(11) | 162.87(9) |
| O3-Mo1-N1 | 156.14(10) | 84.50(9) |
| N1-Mo1-N2 | 71.49(10) | 70.85(8) |
| Mo1-O3-C13 | 136.8(10) | 133.17(10) |
| Mo1-O4-C15 | 124.6(10) | 123.51(10) |
| M1-N1-C5-C6 (torsion angle) | 4.70 | 6.52 |

*2.4. Oxo-transfer reactions*

Stoichiometric as well as catalytic oxotransfer from suitable oxygen atom donors to phosphines of varying basicity are standard reactions for assessment of the reactivity of oxomolybdenum(VI) complexes [15, 33-35]. In this investigation, the oxidation of triphenyl phosphine by DMSO was examined (Eq 1).

$$Ph_3P + Me_2SO \longrightarrow Ph_3PO + Me_2S \quad (1)$$

The ability of **1** to catalyse oxidation of $PPh_3$ was studied in a DMSO-$d_6$ solution in order to facilitate monitoring of the reaction via NMR. When **1** and 8 equivalents of $PPh_3$ were dissolved in deuterated DMSO at room temperature, an instant reaction was observed as the color of the solution changed from yellow to red or dark purple. The yellow color of **1** is attributed to a ligand(pπ)-Mo(dπ) LMCT transition ($\lambda_{max}$ = 365 nm, Fig. **S1**). The initial red

color that is observed in the reaction with $PPh_3$ is attributed to the formation of a Mo(IV) complex, but this complex was found to be too unstable to be isolated. This Mo(IV) oxo species may be oxidized by DMSO to the original Mo(VI) species, or it may react with the Mo(VI) species to form a (purple) $Mo^V$-O-$Mo^V$ dimer [32]. The purple color is due to an absorption at 522 nm (Fig. **S2**), which is the characteristic region for $Mo^V$-O-$Mo^V$ complexes [36]. At 50 °C, the transition from $PPh_3$ to $OPPh_3$ was clearly seen by $^{31}P$ NMR NMR. After a two-hour reaction, two equivalents of $OPPh_3$ were formed, which indicates that DMSO is the ultimate oxidant.

Complex **1** was also studied as a catalyst for the epoxidation of *cis*-cyclooctene, using *t*BuOOH as the oxidant. Optimization of the reaction conditions led to the reactions being run in 1,2-dichloroethane solutions using **1**, *t*BuOOH and *cis*-cyclooctene in a ratio of 1:400:320 and the reaction mixtures were analyzed by $^1H$ NMR. At room temperature, the epoxidation reaction was selective but slow (turn-over frequency, TOF = 30 $h^{-1}$), but at 60 °C it was considerably more rapid (TOF = 134 $h^{-1}$) showing selective oxidation of *cis*-cyclooctene to the epoxide. Control experiments performed in the absence of complex **1** showed no olefin conversion. The catalytic reactions commenced instantly without any noticeable induction times. This epoxidation activity is comparable to that of several other dioxomolybdenum(VI) complexes under related conditions, *e.g.* $[MoO_2(OSiPh_3)(2,2'\text{-bipyridine})]$, [37] $[MoO_2Cl(HC(bim)_3)]Cl$ ($HC(bim)_3$ = tris(benzimidazolyl)methane) [38] and $[MoO_2(acac)(^RN,O)]$ ($^RN$,OH = imino-alcohol derivative of α-pinene) [39].

## 3. Conclusions

The tripodal tetradentate ligand precursor *N*-(2-hydroxybenzyl)-*N*-(2-picolyl)glycine ($H_2$papy) reacts with different dioxomolybdenum(VI) sources to form $[MoO_2(papy)]$ **1** as a mixture of two configurational isomers. These two isomers, *cis*-**1** and *trans*-**1**, can be isolated as crystalline solids using different crystallisation solvents. Variable temperature $^1H$ NMR analysis indicates that while *cis*-**1** is the dominant species in a solution, at lower temperatures the *cis*/*trans* ratio decreases slightly; these observations are in accordance with the *cis* isomer being the kinetically favoured (and, presumably, kinetically trapped) isomer, and the *trans* isomer being the thermodynamically favoured form. DFT calculations conducted in the presence of MeCN using the continuum polarization model (PCM) affords a reasonable value for $K_{eq}$ for the *trans* ⇌ *cis* equilibrium. The rapid equilibration between the two isomers occurs via a Ray-Dutt twist process with a calculated activation barrier of 14.5 kcal/mol. Complex **1**

shows catalytic activity in oxotransfer reactions. The complex effects oxo transfer reaction between $PPh_3$ and DMSO at 50 °C. While the indications of the formation of an Mo(IV) mono-oxo species were detected upon oxo transfer, it was not possible to isolate such a species for further characterization. Also, **1** catalyses the selective epoxidation of *cis*-cyclooctene with *tert*-butyl hydroperoxide as an oxidant with a reasonable activity (TOF = 134 $h^{-1}$) at 60 °C.

## 4. Experimental

### *4.1. Materials and methods*

The starting materials $[MoO_2(acac)_2]$, [40] $[MoO_2Cl_2(dmso)_2]$, [41] $[MoO_2Cl_2(dmf)_2]$, [42] $[MoO_2(S_2NEt_2)_2]$ [43] and $H_2$papy [44] were prepared according to literature procedures. All solvents were of at least 99.5 % purity and used as received, except $CH_2Cl_2$, which was kept over 4 Å molecular sieves and methanol, which was kept over 3 Å molecular sieves. All other chemicals were used as received without any further purification. The reagents were purchased from Sigma-Aldrich. NMR spectra were recorded using a Varian Inova 500 MHz instrument, with standard settings for the $^1H$ nuclei, using deuterated chloroform, methanol, dimethyl sulfoxide, and acetonitrile as solvents, and referenced to the residual signal of the solvent. Infrared spectra were recorded as dry KBr pellets on a Nicolet Avatar 360 FT-IR instrument or a Bruker Vertex 70 with an ATR setup. UV-vis spectroscopy measurements were performed on a Varian 300 Bio spectrophotometer. Mass spectrometry was performed with a Waters ZQ 4000 spectrometer using calibrant as CsI. Results are denoted as cationic mass peaks; unit is the mass/charge ratio.

### *4.2. Synthesis of $[MoO_2(papy)]$ (**1**)*

Finely ground $[MoO_2Cl_2(dmso)_2]$ was added to a solution of (0.200 g, 0.735 mmol) $H_2$papy with two equivalents of triethylamine (1.470 mmol, 204 µL) in 10 mL of methanol. The resulting yellow reaction mixture was stirred overnight, during that time a light yellowish precipitate appeared. The precipitate was removed by a filtration through a pad of Celite, and the filtrate was evaporated in a vacuum to obtain a yellow solid. The solid was analyzed by NMR and was found to be a mixture of two isomers. Individual X-ray quality single crystals of separated isomers were grown as yellow crystals upon slow evaporation of solvent mixtures, *i.e.* methanol (*cis*-**1**), dichloromethane-hexane (*trans*-**1**) or chloroform-diethyl ether (*cis*-**1** and

*trans*-**1** in the same crystal structure) at room temperature. Dissolution of isomerically pure *cis*-**1** or *trans*-**1** led to isomeric mixtures in solution, as detected by $^{1}$H NMR spectroscopy. All attempts to separate the isomeric mixture by column chromatography were unsuccessful. Yield: 0.085 g (35%) $^{1}$H NMR (500 MHz, $CD_3CN$, ppm) (bold letters shows shifts for *trans*-**1**): $\delta$ = 9.12 (d, $J$ = 5.4 Hz, 1H, H-10), **8.67 (d, $J$ = 5.4 Hz, 1H, H-10)**, **8.22 (td, $J$ = 7.8, 1.5 Hz, 1H, H-12),** 7.89 (td, $J$ = 7.8, 1.5 Hz, 1H, H-12), **7.77 (d, $J$ = 7.8 Hz, 1H, H-13), 7.68 (t, $J$ = 6.65, 1H, H-11),** 7.53 (t, $J$ = 6.65, 1H, H-11), **7.39-7.33 (m, 2H, H-5, H-7),** 7.25 (d, $J$ = 7.8, 1H, H-13), 7.20 (d, $J$ = 7.8, 1H, H-7), 7.12 (td, $J$ = 7.8, 1.5 Hz, 1H, H-5), **7.09 (d, 1H, $J$ = 7.8 Hz, H-4), 7.01 (t, $J$ = 6.65, 1H, H-6),** 6.94 (t, $J$ = 6.65, 1H, H-6), 6.54 (d, $J$ = 7.8, 1H, H-4), **5.15 (d, $J$ = 15.1, 1H, H-1a),** 5.06 (d, $J$ = 15.1, 1H, H-1a), 4.97 (d, $J$ = 15.1, 1H, H-2a), 4.52 (d, $J$ = 15.1, 1H, H-2b), 4.46 (d, $J$ = 15.1, 1H, H-3a), **4.35 (d, $J$ = 15.1, 1H, H-2a)**, 4.31 (d, $J$ = 15.1, 1H, H-1b), **4.15 (d, $J$ = 15.1, 1H, H-1b)**, **4.12 (d, $J$ = 15.1, 1H, H-2b),** 3.90 (d, $J$ = 15.1, 1H, H-3b), **3.58 (d, $J$ = 15.1, 1H, H-3a)**, **3.22 (d, $J$ = 15.1, 1H, H-3b)**. $^{13}$C NMR (126 MHz, $CD_3CN$, ppm) $\delta$ = 172.46, 160.62 (-CO-), 160.34, 159.86, 155.96, 154.20, 152.62, 150.28, 142.86, 140.75, 132.09, 131.59, 130.75, 130.22, 129.68, 126.62, 125.07, 124.80, 122.93, 122.87, 122.45, 122.38, 122.11, 117.30 (Ar-C), 65.45, 64.99, 61.58, 61.48, 60.18, 58.46 ($CH_2$). Selected FT-IR ($cm^{-1}$) 929s (Mo=O), 916s (Mo=O). UV-vis in $CH_3CN$: $\lambda_{max}$, nm ($\varepsilon$, $M^{-1}cm^{-1}$): 278 (10082), 365 (3759). ESI-MS: *m/z* = 823 [2x**1**+Na]$^{+}$, 423 [**1**+Na]$^{+}$, 401 [**1**+H]$^{+}$.

*4.3. Oxotransfer studies*

Complex **1** (3.1 mg, 0.0072 mmol) and 8 equivalents of $PPh_3$ (15 mg, 0.0572 mmol) were dissolved in 0.5 mL of DMSO-$d_6$ and the mixture was shaken vigorously for 1 minute to ensure complete dissolution. An instant reaction was noticeable as the color changed from yellow to red or dark purple. The reaction was carried out at 50 °C while the reaction course was monitored by $^{31}$P NMR.

*4.4. Catalytic epoxidation*

Complex **1** was studied as a catalyst for the epoxidation reaction of *cis*-cyclooctene with *t*BuOOH. The reaction was run in a 1,2-dichloroethane solution using **1**, *tert*-BuOOH and *cis*-cyclooctene in a ratio of 1:400:320. The final concentration of the catalyst was *ca.* 0.5 mM. The reaction mixture was analyzed by $^{1}$H NMR after two hours.

*4.5. Crystallography*

X-ray crystallographic measurements were carried out at 170 K (*cis*-**1** and *trans*-**1**) or at 100 K (*cis*-*trans*-**1**) according to the ω-scan method on a Nonius KappaCCD diffractometer using Mo-Kα radiation (λ= 0.71073 Å). The Denzo Scalepack or EvalCCD program packages were used for cell refinements and data reductions. The structure was solved by direct methods, using SHELXS-97 [45] or SIR97 [46] programs with the WinGX [47] graphical user interface. A semi-empirical absorption correction (SADABS [48] or SHELXTL [49]) was applied to all data. Structural refinements were carried out using SHELXS-97.

*4.6. Computational details and modelling*

All DFT calculations were carried out with the Gaussian 09 package of programs [50] using M06 as the hybrid functional [51]. This functional was chosen because it best reproduced the *cis*-**1** and *trans*-**1** equilibrium ratio recorded in the $^{1}$H NMR spectrum at room temperature. The molybdenum atom was described with the Stuttgart−Dresden effective core potential and SDD basis set, [52] and the 6-31G(d′) basis set was employed for all remaining atoms [53]. The reported structures were fully optimized with solvent effect corrections using the available integral equation formalism model (IEFPCM) in the Gaussian 09 suite of programs. The $^{1}$H NMR chemical shifts of the pyridyl α-hydrogen in *cis*-**1** and *trans*-**1** were computed at the above level of theory using the GAIO method available in the Gaussian 09 suite of programs. All reported geometries were fully optimized, and analytical second derivatives were evaluated at each stationary point to verify whether the geometry was an energy minimum (positive eigenvalues) or a transition structure (one negative eigenvalue). Unscaled vibrational frequencies were used to make zero-point and thermal corrections to the electronic energies. The resulting potential energies and enthalpies are reported in kcal/mol relative to the specified standard. Intrinsic reaction coordinate (IRC) calculations were performed to confirm the unequivocal reactant and product species associated with the transition-state structure **TSAB**. The geometry-optimized structures have been drawn with the *JIMP*2 molecular visualization and manipulation program [54].

**Acknowledgements**

This research has been carried out within the framework of COST Action CM1003. MKH thanks the European Commission for an Erasmus Mundus predoctoral fellowship. MGR thanks the Robert A. Welch Foundation (Grant B-1093-MGR). Computational resources through the High Performance Computing Services and CASCaM at the University of North Texas are acknowledged. We also thank Dr. Göran Carlström (Lund University) for assistance with NMR measurements.

**Appendix A. Supplementary data**

CCDC 1502861-1502863 contains the supplementary crystallographic data for *cis*-**1** *trans*-**1** and *cis-trans*-**1**. These data can be obtained free of charge via http://www.ccdc.cam.ac.uk/conts/retrieving.html, or from the Cambridge Crystallographic Data Centre, 12 Union Road, Cambridge CB2 1EZ, UK; fax: (+44) 1223-336-033; or e-mail: deposit@ccdc.cam.ac.uk. Supplementary data associated with this article can be found, in the online version.

**References**

[1] R. Mayilmurugan, B.N. Harum, M. Volpe, A.F. Sax, M. Palaniandavar, N.C. Mösch-Zanetti, Chem. Eur. J. 17 (2011) 704.

[2] J.E. Ziegler, G. Du, P.E. Fanwick, M.M. Abu-Omar, Inorg. Chem. 48 (2009) 11290.

[3] J. Pisk, D. Agustin, V. Vrdoljak, R. Poli, Adv. Synth. Catal. 353 (2011) 2910.

[4] J.M. Mitchell, N.S. Finney, J. Am. Chem. Soc. 123 (2001) 862.

[5] Y.-L. Wong, D.K.P. Ng, H.K. Lee, Inorg. Chem. 41 (2002) 5276.

[6] (a) V. Vrdoljak, J. Pisk, D. Agustin, P. Novak, J.P. Vuković, D. Matkovic´-Cˇalogovic, New J. Chem. 38 (2014) 6176; (b) J. Morlot, N. Uyttebroeck, D. Agustin, R. Poli, ChemCatChem 5 (2013) 601; (c) A. Rezaeifard, I. Sheikhshoaie, N. Monadi, M. Alipour, Polyhedron 29 (2010) 2703.

[7] M.A. Katkar, S.N. Rao, H.D. Juneja, RSC Adv. 2 (2012) 8071.

[8] M. Bagherzadeh, M. Amini, H. Parastar, M. Jalali-Heravi, A. Ellern, L.K. Woo, Inorg. Chem. Commun. 20 (2012) 86.

[9] D.L. Trent, in Kirk-Othmer Encyclopedia of Chemical Technology, Wiley, New York, 4th edn, 20 (1996) 271.

[10] (a) S. Huber, M. Cokoja, F.E. Kühn, J. Organomet. Chem. 751 (2014) 25; (b) F. Cavani, J.H. Teles, ChemSusChem 2 (2009) 508; (b) P. Traar, J.A. Schachner, B. Stanje, F. Belaj, N.C. Mösch-Zanetti, J. Mol. Catal. A: Chem. 385 (2014) 54.

[11] (a) A.J. Burke. Coord. Chem. Rev. 252 (2008) 170; (b) K.R. Jain, W.A. Herrmann, F.E. Kühn, Coord. Chem. Rev. 252 (2008) 556.

[12] G. Chahboun, J.A. Brito, B. Royo, M.A. El Amrani, E. Gómez-Bengoa, M.E.G. Mosquera, T. Cuenca, E. Royo, Eur. J. Inorg. Chem. (2012) 2940.

[13] K.E. Cantwell, P.E. Fanwick, M.M. Abu-Omar, ACS Omega 2 (2017) 1778.

[14] F.E. Kühn, A.M. Santos, M. Abrantes, Chem. Rev. 106 (2006) 2455.

[15] For recent reviews, see for example, R. Hille, R. Mendel, Coord. Chem. Rev. 255 (2011) 991.

[16] (a) R. Hille, J. Hall, P. Basu, Chem. Rev. 114 (2014) 3963; (b) R. Hille, Dalton Trans. 42 (2013) 3029; (c) R. Hille, Chem. Rev. 96 (1996) 2757.

[17] J.H. Enemark, M.M. Cosper, Metal Ions in Biological Systems, 39 (2002) 621.

[18] C. Schulzke, Eur. J. Inorg. Chem. (2011) 1189.

[19] A. Günyar, D. Betz, M. Drees, E. Herdtweck, F.E. Kühn, J. Mol. Catal. A: Chem. 331 (2010) 117.

[20] (a) Y. Wong, L.H. Tong, J.R. Dilworth, D.K.P. Ng, H.K. Lee, Dalton Trans. 39 (2010) 4602; (b) Y. Wong, Q. Yang, Z. Zhou, H.K. Lee, T.C.W. Mak, D.K.P. Ng, New J. Chem. 25 (2001) 353; (c) Y. Wong, J. Ma, W. Law, Y. Yan, W. Wong, Z. Zhang, T.C.W. Mak, D.K.P. Ng, Eur. J. Inorg. Chem. (1999) 313.

[21] K. Unoura, M. Kondo, A. Nagasawa, M. Kanesato, H. Sakiyama, A. Oyama, H. Horiuchi, E. Nishida, T. Kondo, Inorg. Chim. Acta 357 (2004) 1265.

[22] J.P. Donahue, C. Lorber, E. Nordlander, R.H. Holm, J. Am. Chem. Soc. 120 (1998) 3259.

[23] A. Thapper, J.P. Donahue, K.B Musgrave, M.W. Willer, E. Nordlander, B. Hedman, K.O. Hodgson, R.H. Holm, Inorg. Chem. 38 (1999) 4104.

[24] A. Thapper, C. Lorber, J. Fryxelius, A. Behrens, E. Nordlander, J. Inorg. Biochem. 79 (2000) 67.

[25] R. H. Holm, Coord. Chem. Rev. 100 (1990) 183.

[26] K. Dreisch, C. Andersson, C. Stålhandske, Polyhedron 12 (1993) 303.

[27] (a) M.K. Hossain, M. Haukka, R. Sillanpää, D.A. Hrovat, M.G. Richmond, E. Nordlander, A. Lehtonen, Dalton Trans. 46 (2017) 7051; (b) M.K. Hossain, J.A. Schachner, M. Haukka, A. Lehtonen, N.C. Mösch-Zanetti, E. Nordlander, Polyhedron 134 (2017) 275; (c) M.K. Hossain, J.A. Schachner, M. Haukka, N.C. Mösch-Zanetti, E. Nordlander, A. Lehtonen, Inorg. Chim. Acta 486 (2019) 17; (d) A. Peuronen, A. Lehtonen, Top. Catal. 59 (2016) 1132; (e) J.A. Schachner, N.C. Mösch-Zanetti, A. Peuronen, A. Lehtonen, Polyhedron 134 (2017) 73.

[28] A. Lehtonen, R. Sillanpää, Polyhedron 24 (2005) 257.

[29] R. Dinda, P. Sengupta, S. Ghosh, W.S. Sheldrick, Eur. J. Inorg. Chem. (2003) 363.

[30] C.J. Hinshaw, D. Peng, R. Singh, J.T. Spence, J.H. Enemark, M. Bruck, J. Kristofzski, S.L. Merbs, R.B. Ortega, P.A. Wexler, Inorg. Chem. 28 (1989) 4483.

[31] M.R. McDewitt, A.W. Addison, E. Sinn, L.K. Thompson, Inorg. Chem. 29 (1990) 3425.

[32] A. Thapper, A. Behrens, J. Fryxelius, M.H. Johansson, F. Prestopino, M. Czaun, D. Rehder, E. Nordlander, Dalton Trans. (2005) 3566.

[33] (a) A.C. Ghosh, P.P. Samuel, C. Schulzke, Dalton Trans. 46 (2017) 7523; (b) A. Lehtonen, M. Wasberg, R. Sillanpää, Polyhedron 25 (2006) 767; (c) A.J. Millar, C.J. Doonan, P.D. Smith, V.N. Nemykin, P. Basu, C.G. Young, Chem. Eur. J. 11 (2005) 3255; (d) J.T. Hoffman, S. Einwaechter, B.S. Chohan, P. Basu, C.J. Carrano, Inorg. Chem. 43 (2004) 7573.

[34] C. Lorber, M.R. Plutino, L.I. Elding, E. Nordlander, J. Chem. Soc., Dalton Trans. (1997) 3997.

[35] B.E. Schultz, S.F. Gheller, M.C. Muetterties, M.J. Scott, R.H. Holm, J. Am. Chem. Soc. 115 (1993) 2714.

[36] S. Yu, R.H. Holm, Inorg. Chem. 28 (1989) 4385.

[37] A. Rezaeifard, M. Jafarpour, H. Raissi, M. Alipour, H. Stoeckli-Evans, Z. Anorg. Allg. Chem. 638 (2012) 1023.

[38] S. Gago, S.S. Balula, S. Figueiredo, A.D. Lopes, A.A. Valente, M. Pillinger, I.S. Gonçalves, Appl. Catal. A. Gen. 372 (2010) 67.

[39] G. Chahboun, J.A. Brito, B. Royo, M.A. El Amrani, E. Gómez-Bengoa, M.E.G. Mosquera, T. Cuenca, E. Royo, Eur. J. Inorg. Chem. (2012) 2940.

[40] G.J.-J. Chen, J.W. McDonald, W.E. Newton, Inorg. Chem. 15 (1976) 2612.

[41] F.J. Arnáiz, R. Aguado, M.R. Pedrosa, A. De Cian, Inorg. Chim. Acta 347 (2003) 33.

[42] F.J. Arnaiz, R. Aguado, J. Sanz-Aparicio, M. Marinez-Ripoli, Polyhedron 13 (1994) 2745.

[43] W. Adam, R.M. Bargon, S.G. Bosio, W.A. Schenk, D. Stalke, J. Org. Chem. 67 (2002) 7037.

[44] R. Gorkum, J. Berding, D.M. Tooke, A.L. Spek, J. Reedijk, E. Bouwman, J. Catal. 252 (2007) 110.

[45] G.M. Sheldrick, Acta Cryst. A 64 (2008) 112.

[46] A. Altomare, M.C. Burla, M.C. Camalli, C. Giacovazzo, A. Guagliardi, A.G.G. Moliterni, G. Polidori, R. Spagna, J. Appl. Crystallogr. 32 (1999) 115.

[47] L.J. Farrugia, J. Appl. Crystallogr. 32 (1999) 837.

[48] G.M. Sheldrick, SADABS, Bruker Nonius Scaling and Absorption Correction, v 2.10, Bruker AXS, Inc., Madison, WI, USA, 2003.

[49] G.M. Sheldrick, SHELXTL, Bruker Analytical X-ray Systems, Bruker AXS, Inc., Madison, WI, USA, 2005.

[50] Frisch, M. J. et al., Gaussian 09, Revision E.01, Gaussian, Inc., Wallingford, CT, USA, 2009.

[51] (a) Y. Zhao, D.G. Truhlar, Acc. Chem. Res. 41 (2008) 157; (b) Y. Zhao, D.G. Truhlar, Theor. Chem. Acc. 120 (2008) 215.

[52] (a) M. Dolg, U. Wedig, H. Stoll, H. Preuss, J. Chem. Phys. 86 (1987) 866; (b) S.P. Walch, C.W. Bauschlicher, J. Chem. Phys. 78 (1983) 4597.

[53] (a) G.A. Petersson, A. Bennett, T.G. Tensfeldt, M.A. Al-Laham, W.A. Shirley, J. Mantzaris, J. Chem. Phys. 89 (1988) 2193; (b) G.A. Petersson, M.A. Al-Laham, J. Chem. Phys. 94 (1991) 6081.

[54] JIMP2, version 0.091, a free program for the visualization and manipulation of molecules: (a) M.B. Hall, R.F. Fenske, Inorg. Chem. 11 (1972) 768; (b) J. Manson, C.E. Webster, M.B. Hall, Texas A&M University, College Station, TX, 2006, http://www.chem.tamu.edu/jimp2/index.html.

**Graphical Abstract - text**

The complex $[MoO_2(papy)_2]$ (**1**) consists of two configurational isomers in solution, with a low barrier for interconversion. Complex **1** catalyzes phosphine oxidation and epoxidation reactions.